6-2022

FABRICATION AND CHARACTERIZATION OF NANOSTRUCTURED HYBRID MATERIALS FOR GAS SENSING APPLICATIONS

Husam H.D AlTakroori

MASTER THESIS NO. 2022:24

College of Science

Department of Physics

FABRICATION AND CHARACTERIZATION OF NANOSTRUCTURED HYBRID MATERIALS FOR GAS SENSING APPLICATIONS.
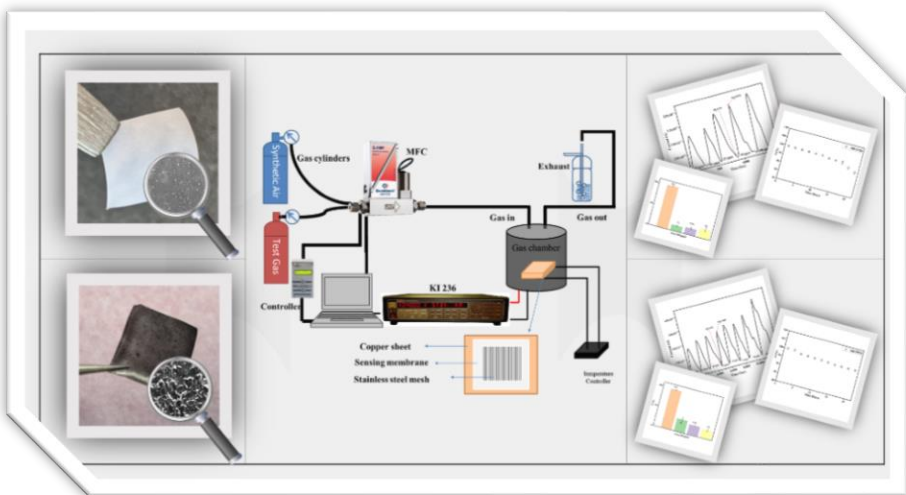
Husam H.D. AlTakroori

June 2022

United Arab Emirates University

College of Science

Department of Physics

FABRICATION AND CHARACTERIZATION OF
NANOSTRUCTURED HYBRID MATERIALS FOR
GAS SENSING APPLICATIONS

Husam H.D. AlTakroori

This thesis is submitted in partial fulfilment of the requirements for the
degree of Master of Science in Physics

June 2022

Cover: Left: the fabricated membranes and their SEM images. Middle: Schematic diagram of the sensor and the experimental setup. Right: The gas sensing performance of the fabricated sensors.

(Photo: By Husam H.D. AlTakroori)

Declaration of Original Work

I, Husam H.D. AlTakroori, the undersigned, a graduate student at the United Arab Emirates University (UAEU), and the author of this thesis entitled "*Fabrication and Characterization of Nanostructured Hybrid Materials for Gas Sensing Applications*", hereby, solemnly declare that this thesis is my own original research work that has been done and prepared by me under the supervision of Professor Saleh Thaker Mahmoud, in the College of Science at UAEU. This work has not previously formed the basis for the award of any academic degree, diploma or a similar title at this or any other university. Any materials borrowed from other sources (whether published or unpublished) and relied upon or included in my thesis have been properly cited and acknowledged in accordance with appropriate academic conventions. I further declare that there is no potential conflict of interest with respect to the research, data collection, authorship, presentation and/or publication of this thesis.

Student's Signature:

Date: ___June 10, 2022_____

Advisory Committee

1) Advisor: Prof. Saleh Thaker Mahmoud

Title: Professor

Department of Physics

College of Science

2) Co-advisor: Prof. Naser Qamhieh

Title: Professor

Department of Physics

College of Science

Approval of the Master Thesis

This Master Thesis is approved by the following Examining Committee Members:

1) Advisor (Committee Chair): Prof. Saleh Thaker Mahmoud
   Title: Professor
   Department of Physics
   College of Science

   Signature   Date   June 10, 2022

2) Member: Prof. Noureddine Amrane
   Title: Professor
   Department of Physics
   College of Science

   Signature   Date   June 10, 2022

3) Member (External Examiner): Dr. Baker Mohammad
   Title: Associate Professor
   Department of Electrical Engineering & Computer Science
   Institution: Khalifa University, UAE

   Signature   Date   June 10, 2022

This Master Thesis is accepted by:

Dean of the College of Science: Professor Maamar Benkraouda

Signature *Maamar Benkraouda*

Date June 22, 2022

Dean of the College of Graduate Studies: Professor Ali Al-Marzouqi

Signature Ali Hassan

Date June 22, 2022

Abstract

The rapid increase in the environmental pollution has become a major concern, and its monitoring has evolved into a priority for human health. This fact has directed the researchers to make more efforts to find new techniques for the detection of gases hazardous to the environment and human health. With the tremendous advances in technology, gas-sensing devices have become popularly used in environmental applications to detect various toxic gases at very low concentrations.

This work aims at developing high-performance gas sensors with enhanced sensitivity, selectivity, low response time, and low operating temperature. The proposed sensors are fabricated based on the integration of nanotechnology and conducting polymer technology. A polymer solution comprised of poly-vinyl alcohol (PVA) and ionic liquid (IL) has been blended once with zinc oxide nanoparticles (ZnO Nps) and another with copper-based metal-organic framework (Cu-MOF) to obtain two distinct flexible membranes. These membranes were assessed for their performance against hazardous gases at room temperature (RT=23°C). The ZnO/PVA/IL and Cu-MOF/PVA/IL membranes showed high sensitivity toward hydrogen sulfide (H_2S) gas with a detection limit of 15 ppm and 1 ppm, and low time response of 24 s and 12 s respectively at RT. Considering this low operating temperature, external heating elements are not required hence the fabrication and operational costs are reduced. The sensors also showed excellent repeatability, long-term stability, and selectivity toward H_2S gas among other gases. Therefore, this study demonstrates the potential of fabricating high-performance gas sensors for monitoring H_2S gas in real-time with high efficiency.

Keywords: H_2S sensor, Metal oxide semiconductor, Metal organic framework, Organic polymer, ZnO NPs, Cu-MOF.

Title and Abstract (in Arabic)

تصنيع ودراسة خصائص المواد الهجينة ذات البنية النانوية لتطبيقات استشعار الغاز

الملخص

أصبح التلوث البيئي المتزايد يشكل مصدر قلق كبير، ومراقبته باتت ضرورة لضمان الحفاظ على صحة الإنسان. هذه الحقيقة قد وجهت الباحثين لبذل المزيد من الجهود لابتكار تقنيات جديدة للكشف عن الغازات الخطرة على البيئة وصحة الإنسان، ومع التقدم الهائل في التكنولوجيا، أصبحت أجهزة استشعار الغاز شائعة الاستخدام في التطبيقات البيئية لاكتشاف الغازات السامة المختلفة بتراكيز منخفضة جدًا.

تهدف هذه الدراسة إلى تطوير مستشعرات غاز ذات حساسية عالية، وزمن استجابة منخفض، ودرجة حرارة تشغيل منخفضة. هذه المستشعرات قد تم تصنيعها بناءً على تكامل تكنولوجيا النانو وتكنولوجيا البوليمر عن طريق مزج كحول عضوي (PVA) معالج بسائل أيوني(IL) ، مع مادتين مختلفتين (ZnO Nps) و (Cu-MOF) للحصول على أغشية مرنة (ZnO/PVA/IL) و(Cu-MOF/PVA/IL) ؛ بهدف استخدامها في تصنيع وتقييم كفاءة أجهزة استشعار الغازات الخطرة في درجة حرارة الغرفة (RT). وقد أظهرت هذه المستشعرات حساسية عالية تجاه غاز كبريتيد الهيدروجين (H_2S) تصل إلى 15 جزء من المليون وزمن استجابة مقداره 24 ثانية في الجهاز الأول (ZnO/PVA/IL)، وحساسية تصل إلى 1 جزء من المليون وزمن استجابة مقداره 12 ثانية في الجهاز الثاني (Cu-MOF/PVA/IL) في درجة حرارة الغرفة.

وما يميز هذه المستشعرات إلى جانب كونها ذات حساسية عالية وزمن استجابة منخفض هي درجة حرارة التشغيل المنخفضة، ما يعني عدم الحاجة إلى أجزاء إضافية لتسخين الجهاز، والذي بدوره يقلل من تكاليف تصنيع وتشغيل الجهاز. وكذلك أظهرت نتائج هذه الدراسة درجة عالية من الانتقائية لغاز كبريتيد الهيدروجين، بالإضافة إلى إمكانية استعمالها بشكل متكرر وبنتائج دقيقة وثابتة على المدى الطويل. وبناءً على ما سبق، فإن هذه الدراسة تقدم نتائج جديدة تمكن من تصنيع مستشعرات غاز عالية الأداء للكشف عن غاز كبريتيد الهيدروجين بكفاءة عالية

مفاهيم البحث الرئيسية: مستشعر لغاز كبريتيد الهيدروجين، أكسيد معدني شبه موصل، هيكل فلزي عضوي، بوليمر عضوي، جزيئات أكسيد الزنك النانوية، هيكل فلزي عضوي نحاسي

Author Profile

Husam AlTakroori received his bachelor's degree in applied physics and an educational diploma in science from Palestine Polytechnic university, Palestine. He is currently a research assistant at United Arab Emirates University, UAE. Before that, he worked as a physics teacher at the Kuwaiti ministry of education for three years.

Acknowledgements

"All praise is for Allah, the lord of the worlds"

First and foremost, I would like to extend my gratitude and appreciation to my advisor, Prof. Saleh Thaker, for his continuous support and guidance, and for his patience and motivation from the first day that I started working with him. I sincerely believe that without his great efforts, this work would have not been accomplished.

My gratitude and appreciation are also extended to Dr. Ashraf Ali, who steered me in the right direction of research activities and filled my knowledge gaps in this field, in addition to his continuous encouragement, invaluable guidance, and precious support blended in a friendly environment.

My sincere thanks as well to Prof. Yaser Greish from the Chemistry Department and my co-advisor Prof. Naser Qamhieh for their help, guidance, and valuable discussions, and for the physics lab specialist Mr. Abdul Razack Hajamohideen for his help and support.

It is a pleasure to thank the Physics Department members including department Chair, faculty and staff for their support and providing me with the valuable and advanced knowledge during my study.

Finally, I would like to acknowledge my beloved parents and my three brothers for their prayers, support, and motivation that they provided, and still provide in everyday of my life. And to all those who provided their help and support, but their names are not mentioned, to all of you, thank you very much.

Dedication

To my beloved parents and brothers

Table of Contents

List of Tables

List of Figures

List of Abbreviations

DW	Distilled Water
EDX	Energy- Dispersive X-ray
FTIR	Fourier Transform Infrared
IL	Ionic Liquid
JCPDS	Joint Committee on Powder Diffraction Standards
LabVIEW	Laboratory Virtual Instrument Engineering Workbench
MFC	Mass Flow Controllers
MOF	Metal Organic Framework
MOS	Metal Oxide Semiconductor
NPs	Nanoparticles
PVA	Poly (Vinyl Alcohol)
PXRD	Powder X-Ray Diffraction
QCM	Quartz Crystal Microbalance
RPM	Round Per Minute
RT	Room Temperature
SAW	Surface Acoustic Wave
SEM	Scanning Electron Microscope
TGA	Thermogravimetric Analysis
VOCs	Volatile Organic Compounds

Chapter 1

Chapter 1: Introduction

1.1 Overview

This work aims at developing an organic-inorganic hybrid gas sensor, by fabricating novel membranes and investigating their sensing capabilities toward H_2S gas among other hazardous gases.

This thesis begins by outlining the problem we are trying to tackle, then states the objectives of this research, and finally reviews the relevant reported literature. Chapter 2 explains the methods used to synthesize, fabricate, and characterize the proposed sensors. Results are presented in chapter 3 followed by a discussion regarding the gas sensing mechanism. In the end, the outcome of this work is concluded in chapter 4.

1.2 Statement of the Problem

There is an inseparable bond between health and the environment. Humans depend on the environment for their survival. Therefore, its monitoring has become a priority for the health of mankind. The Oil and gas industry, road transport, and other industrial sectors are the biggest contributors to air pollution. Several toxic, hazardous, and flammable gases such as Hydrogen sulfide, Hydrogen, Carbon monoxide, and Nitrogen oxide are produced by the above sectors.

Enormous efforts have been invested in tackling this situation by developing gas sensors that are highly sensitive, selective, and stable toward the target gases among others (Joshi et al., 2018; Kohl, 2001; Varghese et al., 2015; J. Zhang et al., 2017).

Hydrogen sulfide (H_2S) has been considered a health concern due to its high toxicity which can harm several systems of the body. In addition

to that, exposure to high concentrations may lead to brain damage or sudden death among workers in fields where this gas is produced.

The demand for a suitable H_2S detector has been raised. Although H_2S sensors are available commercially, they still have some limitations such as high-power consumption, high cost, and long response time. These reasons and others motivated scientists to develop gas sensors that can measure and detect H_2S at low concentrations taking into consideration some important parameters like power consumption, fabrication cost, stability, response time, and selectivity.

That's why, efforts are focused on investigating different materials to fabricate flexible, inexpensive, sensitive, and low power consumption H_2S gas sensors that could be implanted into electronic devices for potentially monitoring harmful gases in real-time with high efficiency.

1.3 Research Objectives

The aim of this work is to develop high-performance and low-power consumption sensors that can be utilized to control environmental pollution by monitoring hazardous gases. The fabricated sensors will use inorganic nanoparticles and metal-organic frameworks embedded separately in organic polymer doped with an ionic liquid to study their gas sensing properties.

Therefore, the objectives of this research are:

1) To synthesize and characterize flexible mixed matrix membranes blended with Zinc oxide nanoparticles or Copper metal- organic framework.

2) To Fabricate gas sensors devices based on the synthesized membranes.

3) To investigate the gas sensing performance of the proposed sensors.

4) To evaluate the potential of the proposed sensors to be deployed in practical industrial applications.

1.4 Relevant Literature

1.4.1 Hydrogen Sulfide

Hydrogen sulfide (H_2S) is one of the most hazardous gases, it was discovered in 1777, and since that time, it has been considered a health concern due to its high toxicity which can harm several systems of the body. That's why, it is included in the lists of toxic and reactive highly hazardous chemicals and is considered to present a potential for a catastrophic event (Occupational Safety and Health Administration). Workers are primarily exposed to H_2S by inhaling it. The concentration of the gas inhaled, and the duration of the exposure are the two factors that symptoms and effects depend on. At low concentrations of about 1.5 parts per million (ppm), H_2S can be smelled like a rotten egg. Prolonged exposure to 2-5 ppm may cause headaches, nausea, and tearing of the eyes. At a concentration of 100 ppm, eye irritation, coughing, and loss of smell may occur after 2-15 minutes, and death may occur after 48 hours. An annihilation of one single breath of high H_2S concentration (over 1000 ppm) may cause immediate death (Occupational Safety and Health Administration).

1.4.2 Types of H_2S Gas Sensors

Gas sensors of various types have been employed to detect H_2S gas, using different principles. Below are some of the most common types:

1.4.2.1 Electrochemical Sensors

Electrochemical sensors have been used since the 1950s to monitor atmospheric gases which then evolved into monitoring H_2S gas by mid 1980s (Ali et al., 2018). The operating principle is governed by the interaction of the target gas with the sensor to produce an electrical signal proportional to the concentration of the gas. Based on the signal produced, the sensor can be further classified into amperometric and potentiometric sensors(Scozzari, 2008; Yourong et al., 2001). The literature demonstrates that both types have been employed for the detection of H_2S gas besides other gases(Liang et al., 2007; Yu et al., 2002). The amperometric sensors which engaged solid or liquid type electrolytes exhibited good sensitivity, repeatability, and fast response times. However, there is a major drawback in these systems which hinders the detection due to the deposition of elemental sulfur in the solid electrolytes(Kramer et al., 2007; Wang & Yan, 2002). Further investigation also revealed that the commercially available solid electrolyte sensors encounter poor selectivity, short shelf life, and limited temperature range (Ali et al., 2018; Yogeswaran & Chen, 2008).

1.4.2.2 Piezoelectric Sensors

The piezoelectric effect has been employed for sensing applications. This technique becomes more popular due to its ability to be utilized at high temperatures (>800°C) (Jiang et al., 2013). Piezoelectric sensors can detect the change of mass resulting from gas adsorption (Wang et al., 2009) and can be categorized, based on their working principle, into Quartz Crystal Microbalance (QCM) sensors and Surface Acoustic Wave (SAW) sensors (Ali et al., 2018). QCM sensors detect the change in mass by measuring the shift of resonant frequency. When the material adsorbs the gas, its mass will increase which decreases the frequency (Nanto et al.,

2000; Pandey et al., 2012). in SAW sensors, however, the change of the material's mass causes travel of Rayleigh wave over the surface. Both types have been used to detect H_2S gas among other gases. In general, sensors fabricated based on this technique have several advantages like linear output, high-frequency response, and small size. However, they have some significant disadvantages such as the small voltage output, the noise of the system, and the temperature compensation which tend to limit their commercial spread. (Zhang & Yu, 2011).

1.4.2.3 Optical Sensors

Optical sensing applications have been widely used for sensing the temperature, magnetic field, and electrical current since the 1970s (Culshaw, 1983). After that, the optical method has been employed in gas sensing because of its high sensitivity, selectivity, and stability (Hodgkinson & Tatam, 2012; Liu et al., 2012). The operating principle is governed by the interaction of light with the analyte. After that, the response is recorded via absorption and emission spectroscopy techniques (Ali et al., 2018). Based on the working technique, optical sensors can be classified into two types: direct sensors, where the analysis is directly detected, and indirect sensors (reagent-mediated sensors), where an intermediate agent is required to modulate the optical response of the analyte (McDonagh et al., 2008; Toda et al., 2004; Varga et al., 2006). Although optical sensors have achieved high sensitivity, they have two main drawbacks that limit their spread which are high cost, and miniaturization (Ali et al., 2018).

1.4.2.4 Chemiresistive Sensors

A chemiresistor is a material that changes its electrical resistance in response to changes in the nearby chemical environment (Banica, 2012).

Recently, chemiresistor technology has been widely used to develop promising sensors for a variety of applications (Lei et al., 2011). Chemiresistive sensors measure the change in the resistance or electrical conductivity when a sensing material is exposed to a target gas. In general, the change in resistance is proportional to the concentration of the target gas; which allows for the amount of the target gas to be measured. This method has attracted much attention due to its high sensitivity, low cost, ease of fabrication, and ability of miniaturization (Majhi et al., 2021).

Several materials that possess chemiresistive properties have been used to detect H_2S gas. Among these materials, metal oxide semiconductor (MOS) materials and metal-organic frameworks (MOFs) have attracted much attention due to their unique properties that promote them to be good candidates for gas sensing applications.

1.4.2.4.1 Metal-Oxide Semiconductor Materials

MOS materials are considered the most commonly and promising materials in gas monitoring system, because of their properties such as their easy and simple fabrication, low limit of detection, fast response time, low cost, and small size. (Ali et al., 2020; COBIANU et al., 2016). However; they are facing some limitations such as high-power consumption, low flexibility, cross-sensitivity, and low stability (Örnek & Karlık, 2012). These limitations pushed researchers to look for solutions to overcome these challenges. Different methods and techniques have been explored to overcome these challenges.

Researchers found that using MOS materials in the nanoscale provides extra advantages, such as low power consumption, repeatability, and the high surface to volume ratio which enhances the chemical reactivity and increases the sensitivity of the sensor (Jiang et al., 1998;

Niranjan et al., 2002; Sciau, 2012). Moreover, it has been found that the incorporation of these inorganic MOS nanomaterials with organic materials provides special characteristics, such as power saving, size compactness, and portability, which would help in achieving the optimum enhancement of gas sensors (Ali et al., 2020). That's why, highly efficient organic sensor devices based on inorganic nanoparticles are currently the focus of active research (Alba-Martin et al., 2012).

Organic polymers, such as poly (vinyl alcohol) (PVA) and chitosan, are characterized by their wide abundance, and their known promising properties, such as flexibility, environmentally friendly, thermal stability, and the ability to form electrolytes by virtue of its hydrophilic nature (Abdullah et al., 2021). Moreover, the electrical conductivity of these polymers can be controlled by doping them with a suitable ionic liquid such as sorbitol, 1-methyl-3-n-decyl-imidazolium bromide, and glycerol (Allam et al., 2013; Ayesh et al., 2012; Josh et al., 2013). Ionic liquids (ILs) are well known for their good ionic conductivity that is attained at room temperature. ILs serve as electrolytes and diffusion barriers, and they have low values of vapor pressure, low toxicity, and are considered environmentally friendly (Abu-Hani et al., 2017; Ayesh et al., 2016). It has been shown that glycerol-IL can be used effectively to control the conductivity of PVA membranes (Ali et al., 2021; Allam et al., 2013). These combined properties can be further exploited by doping the polymer matrix with materials that have an affinity toward the detection of H_2S gas so that changes in their conductivity or resistivity can be recorded.

In 2019, Ali et. al. succeeded in fabricating a low temperature and fast response H_2S gas sensor based on an organic controlled conductivity membrane embedded with tungsten oxide (WO_3) NPs. The sensor comprised of CS-IL-WO_3 showed a good sensitivity of 15 ppm at 40°C,

and a fast response time of 13.6 s (Ali et al., 2020). In another work, Hittini et. al. successfully prepared H_2S gas sensors based on WO_3 NPs embedded in PVA nanofibrous (NFs) membrane containing glycerol IL synthesized through an electrospinning technique. The fabricated sensor showed ultra-sensitivity with a detection limit of 100 ppb at 40°C, and a fast response time of 16.37 s (Hittini et al., 2020).

Zinc oxide (ZnO) is a metal oxide material that possesses a range of physicochemical properties that are apt for hazardous gas sensing applications. It is classified as an n-type II-VI semiconductor with a wide bandgap (3.37 eV), a large excitation binding energy (60 meV), and high electron mobility (400 $cm^2V^{-1}s^{-1}$) (Hsu et al., 2017; Kang et al., 2021). Additionally, ZnO is chemically stable, environmentally friendly, and can be synthesized at a low cost (Diep & Armani, 2016)making it a promising material for the task. The crystalline nature of ZnO allows it to be grown in different structures such as nanoparticles (0D), one-dimensional (1D), two-dimensional (2D), and three-dimensional (3D) structures (B. Zhang et al., 2017). The morphologies such as nanorods, wires, needles, spheres, ellipsoids, and flowers (Zhang et al., 2015)enable controlling the surface area-to-volume ratio, thereby enhancing the utility of the material in a plethora of sensing applications. In addition to that, the bandgap of the material can be altered by doping ZnO with various materials which improves the sensitivity of the sensor with varying operating temperatures (Çolak & Karaköse, 2019; Ghosh et al., 2019; Gupta et al., 2019; Lupan et al., 2017; Navaneethan et al., 2018; Wang et al., 2017; Wei et al., 2020).

The working principle of the ZnO-based sensors is usually evaluated at elevated temperatures of about 300-500°C (Geng et al., 2016; Patil et al., 2016; Xu et al., 2000; Zhu et al., 2018; Zhu & Zeng, 2017). To attain these temperatures external energy has to be provided to the sensor

which would mean an increase in the operational cost. Furthermore, at these temperatures, the flammable and explosive gases are more prone to explosions due to their low ignition point. Additionally, at higher temperatures the stability of the material reduces which would generate inaccurate results (Korotcenkov & Cho, 2012; Park et al., 2013) and this also leads to shortening the lifetime of the sensor. The sensors that are developed to operate at room temperature do not require any additional heating elements, hence their operational cost is reduced, and the risk of explosion is avoided.

1.4.2.4.2 Metal-Organic Frameworks

Metal-organic frameworks (MOFs) are hybrid of organic and inorganic crystalline materials that are composed of positively charged metal nodes surrounded by organic linkers, forming a hollow structure. MOFs have the potential to be deployed as gas sensors due to their unique properties like their high stability, selectivity, and high surface area to volume ratio. (Chen et al., 2021) The advantage of the former property is that it increases the chance of interaction between the sensing material and gas molecules which improves the sensitivity of the material (Pohle et al., 2011). Moreover, it reduces the quantity of material used to fabricate the membrane, which means reducing the thickness of the sensing layer (Hoppe et al., 2018; Park & Kim, 2020; Yao et al., 2020). The high stability and good selectivity also play a crucial role in making this material a good candidate for being deployed in gas sensing applications.

Literature reports a decent amount of interest in Copper MOF (Cu-MOF) among other types. Campbell et al. demonstrated that detection of the sub-ppm level of ammonia vapor can be achieved using conductive Cu-MOF (Campbell, Sheberla, et al., 2015). The same group also demonstrated that Cu-MOF is selective to an array of volatile organic

compounds (VOCs) based on their functional groups (Campbell, Liu, et al., 2015). This is also supported by Smith M K et al. by synthesizing Cu-MOF film onto graphitic electrodes to detect ammonia at sub-ppm level (Smith et al., 2016). Cu-MOF was also used to detect other gases like NO_2 and acetone vapor (Arul et al., 2021; Yao et al., 2017). Different methods were employed to fabricate sensing devices, such as coating MOF on electrodes, using solvated "paste" (Chen et al., 2014), drop-casting (Campbell, Liu, et al., 2015; Campbell, Sheberla, et al., 2015), solvent-free mechanical abrasion (Campbell, Liu, et al., 2015), and in-situ film growth (Smith et al., 2016).

The Solution casting method was used to fabricate an H_2S gas sensor based on CuO NPs embedded within PVA_IL. The sensor was sensitive to H_2S gas with concentrations as low as 10 ppm at 80°C (Ayesh et al., 2016).

The aim of this investigation is to develop an organic-inorganic hybrid gas sensor, where a matrix of PVA/IL polymer is separately doped with ZnO NPs and Cu-MOF to explore their gas sensing capabilities towards H_2S gas among other hazardous gases. To the best of our knowledge, a composite membrane of ZnO/PVA or Cu-MOF/PVA has not been reported for gas detection, so far. The expected low fabrication and operational costs, flexibility, and ability to be operating at room temperature, will enable the device to be deployed in monitoring these threats in real-time application scenarios.

Chapter 2

Chapter 2: Materials and Methods

This chapter is divided into five sections: The first section reviews the materials used to fabricate the sensing membranes. The second section explains the fabrication methods of the Cu-MOF and the membranes. After that, the characterization techniques are mentioned in the third section. Finally, the sensor fabrication and the experimental setup are discussed in the fourth and fifth sections respectively.

2.1 Materials

Zinc oxide (ZnO) nano-powder (<100nm), poly (vinyl alcohol) (PVA) (MW ~ 61,000 Da), glycerol (>99.5%), copper (II) nitrate trihydrate ($Cu(NO_3)_2.3H_2O$), ethanol (EtOH), aqueous ammonia (NH4OH), and 2,3,6,7,10,11-hexahydroxytriphenylene hydrate (H6hhtp) were purchased from Sigma-Aldrich (USA) and were used without further purification.

2.2 Fabrication of the Sensing Membranes

2.2.1 Fabrication of the ZnO/ PVA /IL Membrane

50 mg of ZnO NPs were dispersed in 40 ml of distilled water (DW) using a vortex shaker. After that, 1000 mg of PVA granules were added to the dispersed ZnO NPs and kept under vigorous stirring at 90°C until all the PVA was dissolved in the mixture. After that, the mixture was doped with 1 ml of glycerol and kept under continuous stirring for 20 min. The mixture formed was then cast onto a petri dish and dried in the oven at 70°C for 18 h, resulting in a flexible membrane as shown in Figure 1. The thickness of the membrane was determined to be 200 μm.
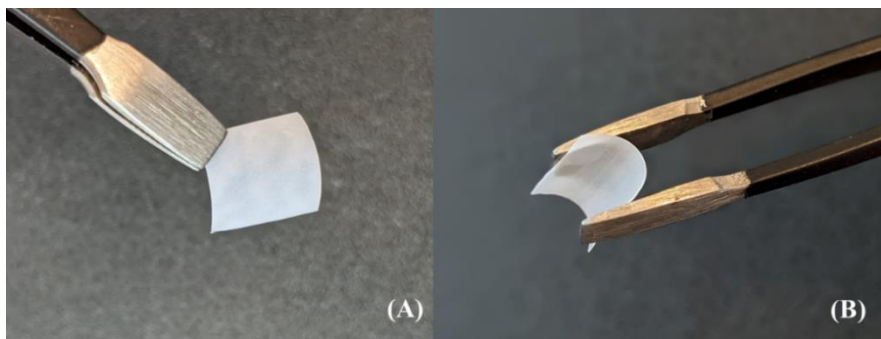
Figure 1: The fabricated ZnO/PVA/IL membrane. (A) 1×1 cm^2 sample of the membrane. (B) Demonstration of its high flexibility

2.2.2 Fabrication of the Cu-MOF/PVA/IL Membrane

Cu-MOF was synthesized in collaboration with the Chemistry Department at UAEU, following a previously reported procedure described by Hoppe et. al. (Hoppe et al., 2018). 2,3,6,7,10,11-hexahydroxytriphenylene hydrate (0.30 mmol, 1 eq.) was added to 8.4 mL of DW in a Pyrex tube to form the first solution. Aside from that in another tube, $Cu(NO_3)_2 \cdot 3H_2O$ (0.53 mmol, 1.75 eq.) was dissolved into 2 mL of DW and 30 eq. of conc. NH_4OH to form the second solution. After that, the second solution was added wisely to the first solution and placed in an oven at 80°C for 24 h. The precipitated black powder was then collected using centrifugation and washed twice with ethanol. Finally, the obtained Cu-MOF was soaked in ethanol for 24 h and dried in a vacuum oven at 80°C for 24 h.

To fabricate the Cu-MOF/PVA/IL membrane, 1.25 mg of Cu-MOF were first dispersed in each ml of DW and stirred for 15 min at 1100 RPM to attain a homogenous dispersion. Aside from that, 5000 mg of PVA granules were dissolved in 100 mL of DW and kept under vigorous stirring at 70°C until a clear and homogenous solution was obtained (Abu-

Hani et al., 2017; Ayesh et al., 2016; Haik et al., 2014). After that, 20 ml of PVA stock solution were doped with 1 ml of glycerol and with Cu-MOF that was suspended in 2.5 mL of DW at 70°C. The mixture formed was then cast onto a petri dish and dried in the oven at 70°C for 16 h, resulting in a flexible membrane as shown in Figure 2. The thickness of the membrane was determined to be 215 μm.
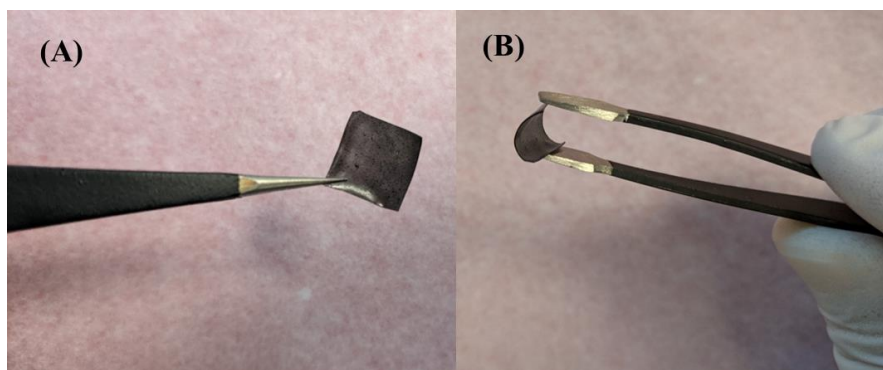
Figure 2: The fabricated Cu-MOF/PVA/IL membrane. (A) 1×1 cm² sample of the membrane. (B) Demonstration of its high flexibility.

2.3 Characterization

ZnO NPs and Cu-MOF powder were subjected to analysis for their structural and morphological characteristics. A powder x-ray diffraction (PXRD) of the as-received ZnO NPs and Cu-MOF powder were performed using a Rigaku, MiniFlex 600-C instrument, USA, with a Cu Kα X-ray with a scan range of 2–80° and at a scan rate of 1°/min. The morphologies of the ZnO NPs, Cu-MOF powder, and the membranes were investigated using a Thermo Scientific Quattro S Scanning electron microscope (SEM) (USA) at an operating voltage of 15 kV. The chemical compositions of the Cu-MOF and the membranes were determined by energy- dispersive X-ray (EDX) spectroscopy apparatus on the same SEM.

The membranes were further analyzed for their composition by Fourier transform infrared (FTIR) spectroscopy using a Thermo Nicolet, NEXUS, 470 FTIR instrument. A KBr disk method over a scan range of 400–4000 cm^{-1} was used. The thermogravimetric analysis (TGA) was recorded using TGA-Q500, TA Instruments, USA with a ramp rate of 20°C/min and within a temperature range of 30–800°C.

2.4 Sensors Fabrication

Each sensor was fabricated by inserting a 1×1 cm^2 piece of each membrane between two electrodes. The bottom electrode is a 1.5×1.5 cm^2 piece of Cu metal plate with a thickness of 0.15 μm, and the top electrode is a 0.8×0.8 cm^2 piece of stainless steel mesh which is resistant to H$_2$S gas with a grid size of 250×250 μm^2. The layers were fixed together with a temperature-resistant Kapton tape (Ali et al., 2021).

2.5 Gas Sensing Experimental Setup

Each sensor was fixed inside a temperature- controlled Teflon chamber on a test stage as illustrated in figure 3(A & B). The test chamber was sealed and placed inside a fume hood to maintain a non-humid atmosphere throughout the measurement. To conduct the test, a mixture of the test gas diluted with synthetic air was introduced into the chamber using Bronkhorst mass flow controllers (MFC). The device was kept at room temperature (23°C) throughout the testing sequences.
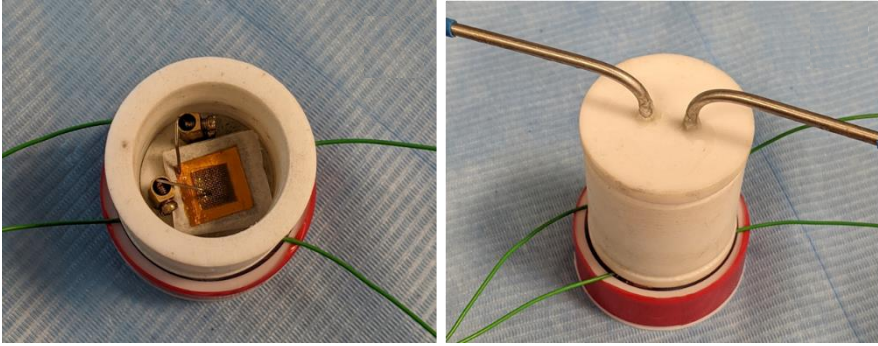
Figure 3: The test chamber with the sensor fixed inside.

Keithley instruments source measurement unit (KI236) was used to record the response of the sensors by measuring the electrical current signal as a function of time at different H_2S gas concentrations.

The sensor response (S%) was calculated using Eq. (1).

$$S\ (\%) = \frac{I_g - I_a}{I_a} \times 100 \tag{1}$$

Where I_a is the reference current when the sensor was exposed to air and I_g is the current measured when the sensor was exposed to H_2S. Furthermore, the sensor's response time was found by calculating the time needed by the sensor to reach 90% of its maximum response.

A constant bias voltage of 4 V and 2.5 V was applied between the electrodes for the ZnO and Cu-MOF devices respectively. LabVIEW software was used to interface and record the response of these units. Figure 4 graphically illustrates the sensor component and the sensing experimental setup.

Figure 4: Schematic diagram of the sensor and the experimental setup.

Chapter 3

Chapter 3: Results and Discussions

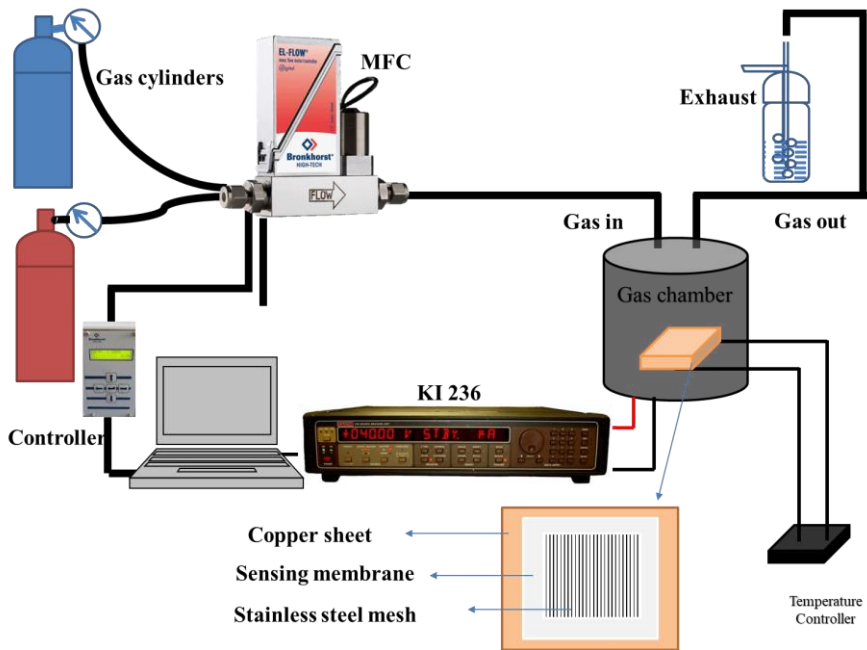This chapter is divided into two sections. The first section discusses the results obtained for the ZnO NPs and ZnO/PVA/ IL membrane, while the second section discusses the results obtained for the Cu-MOF and Cu-MOF/PVA/ IL membrane. In each section, both the powder and the fabricated membrane were first characterized to study their structural and morphological properties. After that, the sensing performance of the membrane was investigated. Finally, the sensing mechanism of the membrane was discussed.

3.1 ZnO NPs and ZnO/PVA/IL Membrane

3.1.1 Structural and Morphological Characterization

Figure 5 shows a comparison between the XRD patterns of the as-received ZnO NPs, the PVA/IL membrane, and the ZnO/ PVA/IL membrane. Compared with the JCPDS pattern of pure ZnO (Card # 36-1451), the as-received ZnO shows a phase-pure composition where all peaks of the standard ZnO were observed. The PVA within the PVA/IL and composite matrices showed two broad peaks at 19.3 and 20.8° (Mashrai et al., 2017; Ristić et al., 2005; Roy et al., 2013; Singh et al., 2008). Additionally, the composite membrane confirmed the presence of the ZnO NPs, where its characteristic peaks representing the 010, 002, and 011 planes were observed.
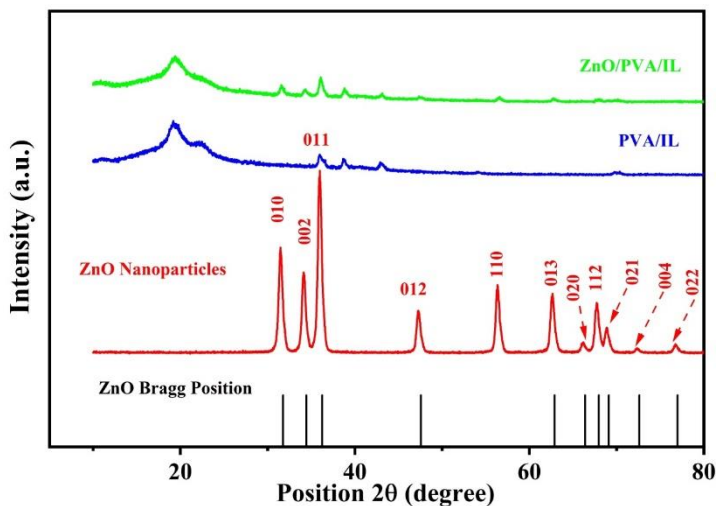
Figure 5: Comparison of XRD pattern for ZnO NPs, PVA/IL membrane and ZnO/PVA/IL composite membrane.

The membrane was subjected to Thermogravimetric Analysis (TGA) as seen in Figure 6(A). From the decomposition curves, we can observe that there is a gradual loss in weight due to the evaporation of water molecules and adsorbed moisture content. Additionally, the loss in weight between 300-550°C is attributed to the removal of organic groups (Mashrai et al., 2017). No appreciable weight loss beyond 700°C was observed, inferring the formation of stable inorganic phases (Rawool & Srivastava, 2019). A slight variation in the thermal profile of the composite membrane was observed, which is because ZnO NPs are thermally stable throughout the heating cycle. The recorded profile matches well with the reported literature (Mashrai et al., 2017) confirming the incorporation of ZnO NPs into the polymer matrix.
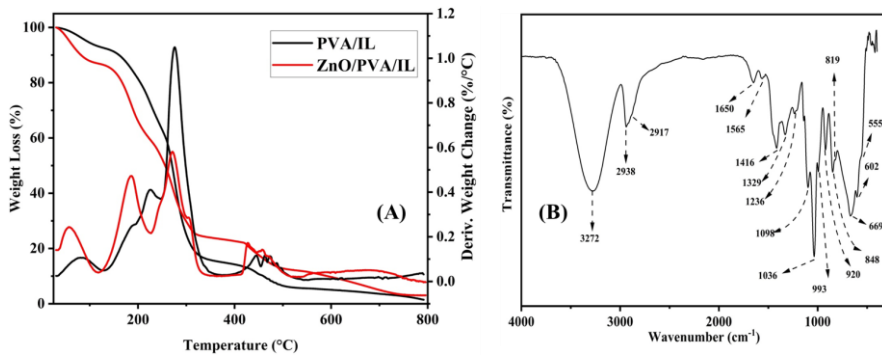
Figure 6: TGA and FTIR characterization. (A) TGA comparison of PVA/IL and ZnO/PVA/IL membranes. (B) FTIR spectra of ZnO/PVA/IL membrane.

The FTIR analysis from Figure 6(B) shows that the membrane has the functional peaks associated with PVA (Ali et al., 2022; Roy et al., 2013) and ZnO NPs (Jayarambabu et al., 2014; Roy et al., 2013) along with a slight shift in their positions inferring the incorporation of the NPs in the polymer matrix. The broad absorption bands at 3272 cm^{-1} and 2938 cm^{-1} denoting the O-H and C-H stretching modes, respectively, are observed. The band at 555 cm^{-1} is attributed to the Zn-O stretching vibration mode (Roy et al., 2013), while the bands at 1142 cm^{-1}, and 1329 cm^{-1} are ascribed to the primary and secondary alcohol in-plane bending modes (Jayarambabu et al., 2014).

Figure 7(A & B) shows the SEM and EDX analysis, respectively of the ZnO/PVA/IL membrane. The image shows a uniform dispersion of the NPs incorporated into the membrane. However, ZnO NPs were observed in the form of agglomerations with a uniform size distribution, which is a common criterion of NPs dispersed in highly viscous PVA solutions. The elemental analysis confirms the presence of Zn and O in the composite membrane.
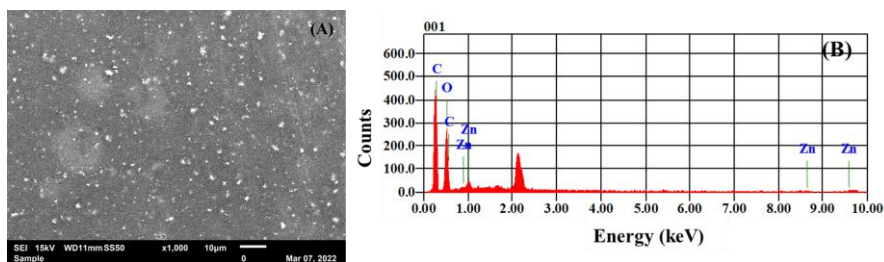
Figure 7: SEM and EDX characterization for the ZnO/PVA/IL membrane. (A) SEM image of the membrane. (B) EDX spectrum of the membrane.

3.1.2 Gas Sensing Performance

The composite membrane sensor was evaluated for its response against H_2S gas exposure at different concentrations with respect to time at room temperature (RT). Figure 8(A) shows the sensor response to different concentrations of H_2S gas over a period of time. Figure 8(B) shows the current response with respect to the test gas concentration.

An increase in the response was observed as a result of increasing the concentration of the test gas. After each exposure to the test gas, the chamber was flushed with synthetic air to remove any residual gas molecules. It is also noted that while the chamber was flushed, the current values were reduced to their starting values in the absence of the test gas demonstrating the reversibility of the sensor.
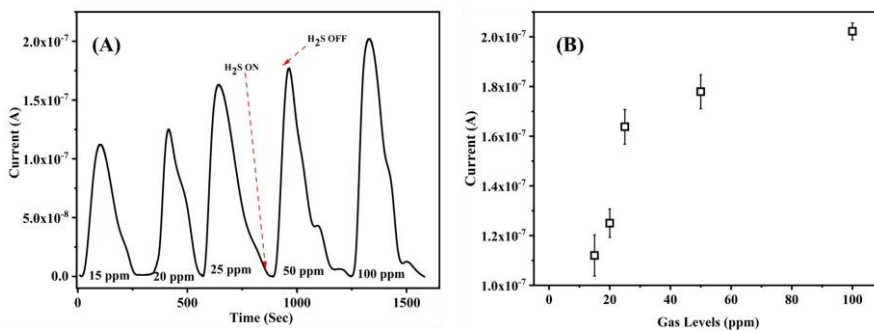
Figure 8: Response of ZnO/PVA/IL membrane to H$_2$S gas. (A) Current response of the membrane to H$_2$S gas exposure at different concentrations with respect to time. (B) The current response of the membrane as a function of gas concentrations.

The sensor was further tested for its repeatability and long-term stability. Figure 9(A) demonstrates excellent repeatability of sensing in the membrane with a near-identical current response for 5 cycles of exposure to H$_2$S gas at a concentration of 100 ppm. Figure 9(B) shows the response of the membrane to 100 ppm of H$_2$S gas exposed for 21 days which demonstrates its long-term stability. It can be seen that the response is in the 94–99% region with minimal error bars.
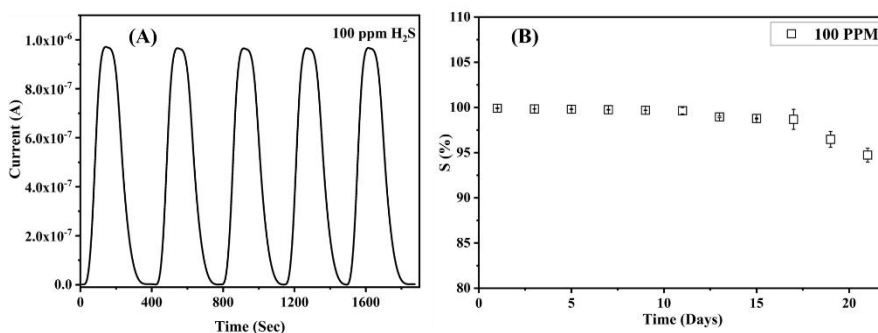
Figure 9: Repeatability and long-term stability of the ZnO /PVA/IL membrane. (A) Repeatability of the membrane at 100 ppm H$_2$S. (B) Long-term stability of the membrane for 21 days at 100 ppm H$_2$S gas.

Furthermore, the sensor's response time was also calculated and found to be 24 s for 100 ppm of H_2S gas at RT.

Finally, the sensor's selectivity was measured by exposing it to 100 ppm of H_2, C_2H_4, and CO gases at RT. Figure 10 illustrates the response of the sensor for those gases, showing a significant difference between the response to H_2S compared to the other gases which indicates an excellent selectivity of the proposed sensor toward those gases.
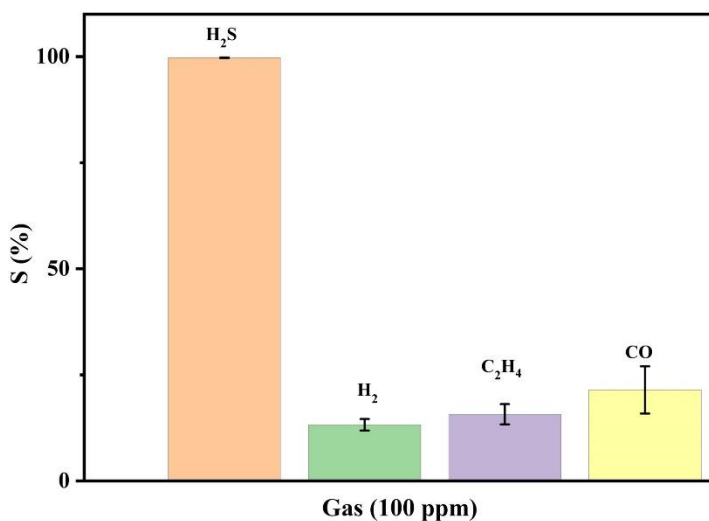
Figure 10: Selectivity of the ZnO/PVA/IL membrane to 100 ppm of H_2S compared to H_2, C_2H_4, CO gases at 100 ppm.

3.1.3 Gas Sensing Mechanism of the ZnO/PVA/IL Membrane

The sensing mechanism of the ZnO/PVA/IL membrane can be elaborated as a surface sensing mechanism (Kang et al., 2021; Wang et al., 2019; Yuan et al., 2019; Zhao et al., 2019), which is based on a process of adsorption-oxidation-desorption. ZnO NPs are embedded into the polymer matrix as seen in figure 7(A) in the form of islands. When flushed with synthetic air, the hydrophilic nature of the matrix allows the oxygen

molecules to get adsorbed on the surface which capture the electrons from the ZnO conduction band making them negatively charged ions (Kang et al., 2021) and thereby providing surface acceptors sites as shown in figure 11(A). Once the polymer has acquired an equilibrium the conductivity of the material reaches a constant state. Upon the exposure to reducing gases such as H_2S, the charge transfer process is initiated by the oxidization of the oxygen anions on the surface which provides the additional free electrons that migrate into the ZnO conduction band as shown in figure 11(B). This reduces the thickness of the depletion layer which gradually reaches equilibrium enhancing the conductivity of the membrane. When the chamber is flushed with synthetic air, the target gas molecules are gradually expelled out from the membrane which reduces the conductivity of the material to the base values recorded.

In addition to that, the homogeneous distribution of the ZnO NPs within the PVA\IL matrix provides an enhanced venue for the mentioned mechanism to take place at room temperature. This can be explained by the extensive H-bonding network that takes place between the -OH groups of the PVA polymeric matrix, as well as the IL. This network facilitates charge transfer across the composite membrane, following the adsorption of the oxygen species from air and their reduction by H_2S in a steam of the latter gas.

Furthermore, based on our findings that sensing was recorded at RT, it indicates that the chemical reaction taking place at the surface dominates the sensing mechanism (Wang et al., 2015). As the oxygen is adsorbed on the surface, a larger surface area of the membrane provides larger active sites for the test gas to interact with the membrane hence the sensitivity towards the target gas was enhanced. At temperatures between 150-300°C, a hybrid mechanism of surface reactivity and gas diffusion

contributes to the sensitivity of the membrane whereas above 300°C the sensitivity is limited to the gas diffusion phenomenon. The equations for the surface adsorption reactions were outlined by Kang et al (Kang et al., 2021). The sensitivity of the membrane reported in the current investigation would be supported by the former.
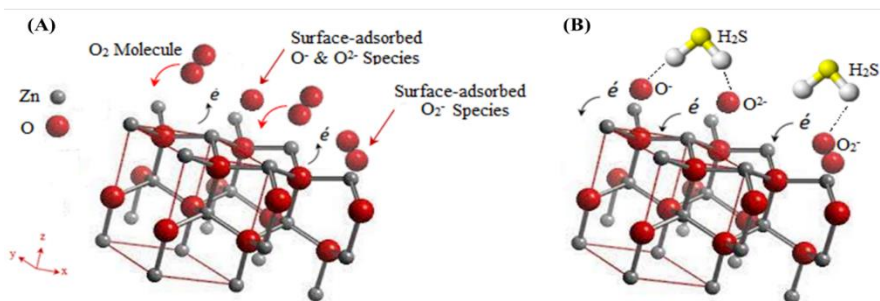
Figure 11: Mechanism of interaction between ZnO crystal lattice and O_2 molecules in (A) air and (B) when flushed with H_2S gas.

3.1.4 A Comparison of the Proposed Sensor Performance with the Reported Literature.

Table 1 demonstrates a comparison between the sensing performance of the fabricated ZnO/PVA/IL sensor and previously reported H_2S sensors based on ZnO material. It can be noticed that ZnO has been used in several structures and doped with different materials to fabricate gas sensors. To evaluate the performance of any sensor, several parameters have to be considered, and the most important are the operating temperature, the detection limit, and the response time. The sensors with lower detection limits than our proposed sensor suffer from high operating temperature. Similarly, sensors that work at room temperature have a higher detection limit than our proposed sensor. Therefore, among these sensors, our proposed sensor has successfully met the expectations by

achieving a low detection limit at low operating temperature with a relatively fast time response. Furthermore, the sensor depicts high flexibility, low cost, easy fabrication, and low-power consumption, which thus holds a great promise for flexible electronic gas sensors.

Table 1: A comparison of the ZnO/PVA/IL sensor performance with the reported literature.

Sensor/Material	Gas	Operating Temp °C	Detection limit (ppm)	Response time (Second)	Reference
ZnO/PVA/IL	H_2S	RT	15	24	This Work
Colloidal ZnO QDs	H_2S	RT	50	16	(B. Zhang et al., 2017)
ZnO/γ Fe_2O_3 Electrochemical	H_2S	RT	250	60	(Ghosh et al., 2017)
Al-ZnO spray pyrolysis	H_2S	200	150	200	(Kolhe et al., 2018)
polyaniline / ZnO hexagonal microdiscs	H_2S	RT	50	63	(Zhang et al., 2019)
Lettuce like ZnO 3D	H_2S	150	100	15	(Yu et al., 2020)
Cu doped ZnO RGO	H_2S	RT	100	14	(Shewale & Yun, 2020)
ZnO ZnS Hetrostructre	H_2S	150	5		(Ding et al., 2020)
ZnO CuO composite	H_2S	40	10	173	(Wang et al., 2020)
ZnO NPs	CO	RT	25		(Narayana et al., 2020)
Dumbbell shaped ZnO 3D	H_2	60	100	20	(Kumar et al., 2020)

3.2 Cu-MOF and Cu-MOF/PVA/IL Membrane

3.2.1 Structural and Morphological Characterization

Figure 12(A) shows a comparison between the PXRD patterns of the Cu-MOF with the simulated pattern, using the lattice parameters from previously reported studies (Nam et al., 2019). Highscore plus software package was used to simulate the pattern, using the said lattice parameters. The Cu-MOF pattern matches well with that reported in the literature, where peaks denoting the XRD diffraction of the 200, 210, 220, 420, and 303 planes were observed. The structural orientation of the Cu-MOF, indicating the linkages between the Cu^{2+} oxo clusters and the HHTP linker molecules, is shown in Figure 12(B). The Cu-MOF exhibits the hierarchical graphene-like 2D structure, which was previously supported by the work of Hoppe et al. (Hoppe et al., 2018). Figure 13 (A) further confirms these morphological characteristics of the Cu-MOF crystallites. Cu-MOF crystallites appear as 2D platelets and flakes, with an average thickness of 150 nm. The selected area of the EDX pattern of the Cu-MOF crystallites, shown in Figure 13(B), indicates the phase purity of the as-prepared Cu-MOF crystallites.
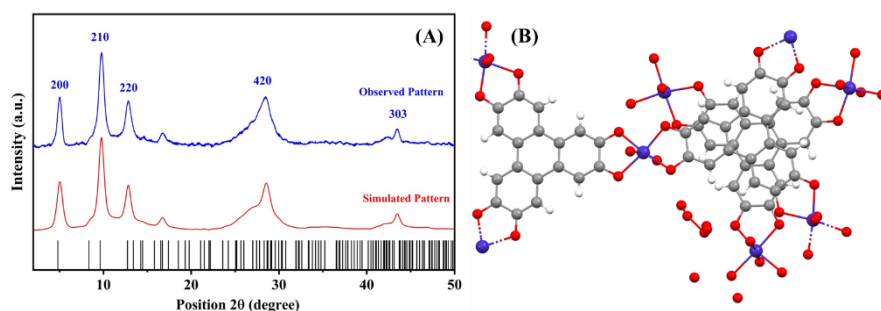

Figure 12: XRD pattern and structural information of the Cu-MOF powder. (A) Comparison of PXRD pattern for the observed and simulated Cu-MOF powder, (B) Structural information of the 2D Cu-MOF.
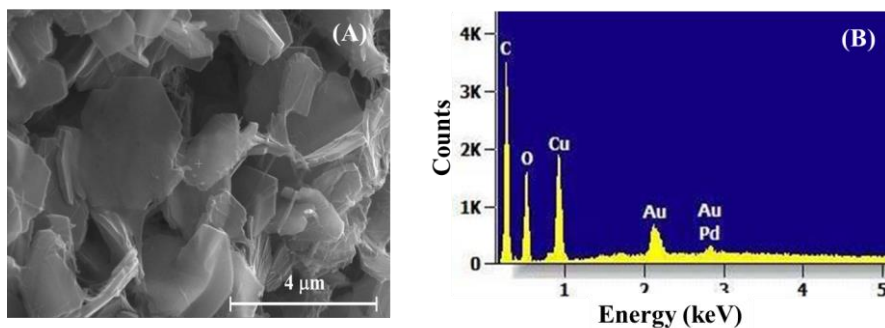
Figure 13: SEM and EDX characterization for the Cu-MOF powder. (A) SEM micrograph, (B) EDX elemental analysis pattern of the Cu-MOF powder.

The Cu-MOF/PVA/IL and Cu-MOF-free PVA/IL membranes were subjected to thermogravimetric analysis (TGA) from room temperature up to 800°C as seen in Figure 14(A). From the decomposition curves, we are able to observe that there is an initial weight loss of around 81.6°C in both materials due to the evaporation of water molecules and adsorbed moisture content. This was followed by a second two-step event, with the first peak at 188.9°C in both samples, while the second peak was observed at 225.5°C for the MOF-free matrix and 215.1°C for the composite membrane. These peaks showed a similar extent of weight loss and denote the evaporation of the remaining organic solvents (Kumar et al., 2013). The third thermal event was observed at 276.5°C for the MOF-free matrix and is related to the breakdown of the PVA polymeric chains. However, a delay in this event has occurred in the composite membrane due to the presence of the Cu-MOF, which was observed at 337.9°C. This is attributed to the extensive removal of the organic content of the composite membrane (MOF linkers; pyromellitic acid, and PVA/IL matrix) (Rawool & Srivastava, 2019). Moreover, the shift in this event could also be used to indicate a chemical stabilization of the polymeric matrix, through extensive H-bonding formation between the highly

functionalized Cu-MOF and the PVA/IL matrix. This has been further confirmed by the presence of a multi-peak thermal event of the MOF-free matrix and the presence of a single event for the composite membrane, as shown in the fourth thermal event. The multi-step weight loss could be related to the successive degradation of the polymeric chains in the MOF-free matrix. On the other hand, the absence of these multi-steps in the thermogram of the composite membrane confirms the stabilization of the matrix by the MOF particles, hence, their degradation takes place as a single thermal event. A final thermal event was observed as a plateau, at a temperature above 550°C, where there was no appreciable weight loss denoting the formation of stable inorganic phases (Rawool & Srivastava, 2019). The profile of the recorded TGA matches well with the literature for Cu-MOF (Arul et al., 2021; Liu et al., 2021), also confirming the incorporation of Cu-MOF in the membrane.

The FTIR analysis in Figure 14(B) shows a similarity between the spectra of the PVA/IL matrix and the composite membrane. This similarity is attributed to the presence of a small proportion of the Cu-MOF, which is below the detection limit of FTIR as a technique (Rawool & Srivastava, 2019).
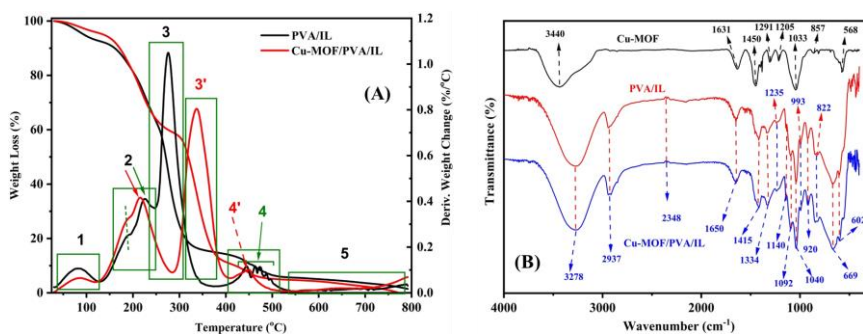
Figure 14: TGA and FTIR characterization. (A) TGA comparison of PVA/IL & Cu-MOF/PVA/IL membranes (B) FTIR spectra of the Cu-MOF powder, PVA/IL, & Cu-MOF/PVA/IL membranes.

Figure 15(A & B) shows the SEM and EDX analysis of the Cu-MOF/PVA/IL membrane. The SEM image shows a uniform distribution of the Cu-MOF 2D platelets. The weak absorption of Cu in the EDX pattern of the composite membrane could be attributed to the coverage of the Cu-MOF platelets within the polymeric matrix, in addition to the presence of Cu-MOF in a small proportion, as compared with the PVA/IL matrix.
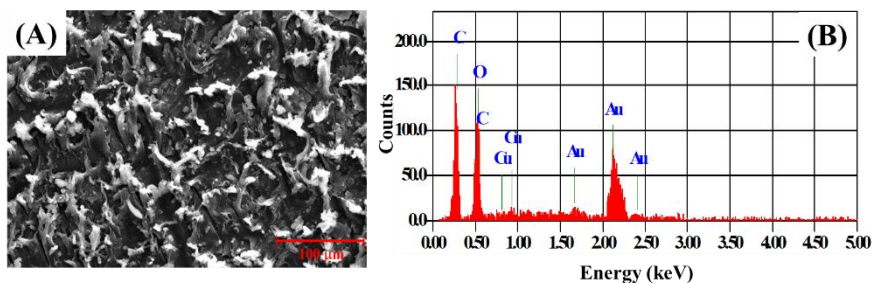
Figure 15: SEM and EDX characterization for the Cu-MOF/PVA/IL membrane. (A) SEM image of the membrane. (B) EDX spectrum of the membrane.

3.2.2 Gas Sensing Performance

The composite membrane sensor was evaluated for its response against H_2S gas exposure at different concentrations with respect to time at RT. Figure 16(A) shows the sensor response to different concentrations of H_2S over a period of time. Figure 16(B) shows the current response with respect to the test gas concentration.
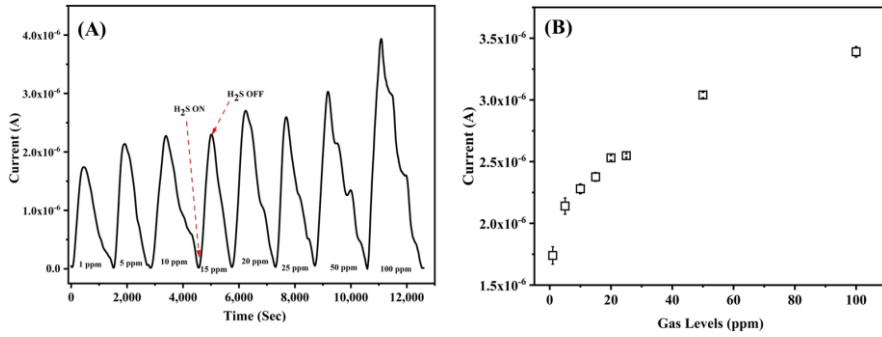
Figure 16: Response of ZnO/PVA/IL membrane to H₂S gas. (A) Current response of the membrane to H₂S gas exposure at different concentrations with respect to time. (B) The current response of the membrane as a function of gas concentrations.

The data show an increase in the measured current signal as a result of increasing the concentration of the test gas. After each exposure to the test gas, the chamber was flushed with synthetic air to remove the adsorbed gas molecules from the sensing membrane before exposure to the next cycle of the target gas. It is also noted that during the flush, the current values gradually reduced to their initial values in the absence of the test gas, demonstrating the reversibility of the sensor.

The sensor was further tested for its repeatability and long-term stability. Figure 17(A) demonstrates excellent repeatability, showing an excellent response for 100 ppm of H₂S gas. Figure 17(B) shows the response of the sensor to 100 ppm of H₂S gas exposed for 21 days which demonstrates its long-term stability. It can be seen that the response is in the 96-99% region, with negligible error bars.
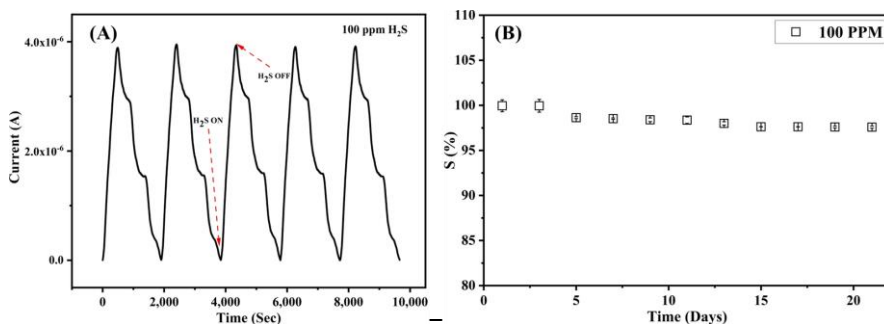
Figure 17: Repeatability and long-term stability of the Cu-MOF/PVA/IL membrane. (A) Repeatability at 100 ppm H_2S. (B) Long-term stability of the membrane for 21 days at 100 ppm H_2S.

Furthermore, the sensor's response time was calculated and found to be 12 s for 100 ppm of H_2S at RT. Finally, the selectivity of the sensor was investigated by exposing it to 100 ppm of H_2, C_2H_4, and CO gases at RT. Figure 18 illustrates the response of the sensor for those gases, showing a significant difference between the response to H_2S compared to other gases which indicates an excellent selectivity of the proposed sensor.
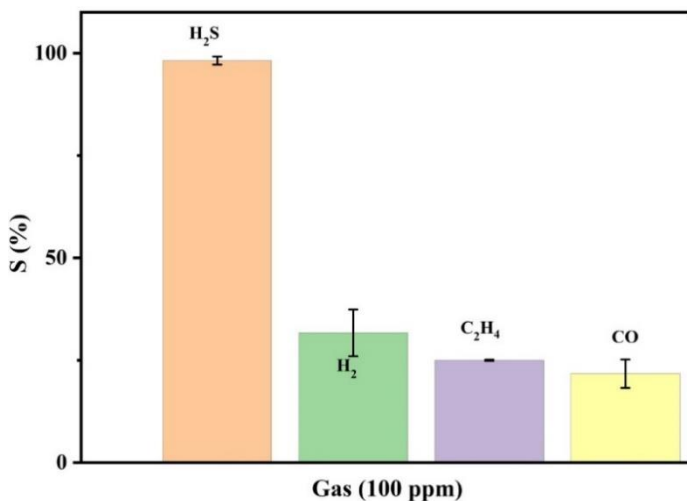
Figure 18: Selectivity of the Cu-MOF/PVA/IL membrane to H_2S in comparison to H_2, C_2H_4, CO gases at 100 ppm at RT.

3.2.3 Gas Sensing Mechanism of the Cu-MOF/PVA/IL Membrane

The polymeric matrix of the Cu-MOF/PVA/IL membrane is hydrophilic in nature, with –OH groups aligned along the chains. The IL is hydrophilic in nature with 3-OH groups along each IL molecule. In the presence of the Cu-MOF2D crystallites, the hydrophilic endings of the HHTP ionized linker contribute to the formation of a network, with an extensive H-bonding along all participating molecules, as illustrated in Figure 19. Upon exposure to the highly acidic H_2S molecules, they contribute to the H-bonded network of molecules, through the attraction of the H_2S-H atoms to the high electron density, along all involved O atoms of the PVA, IL, and the Cu-MOF molecules. Hence, the transfer of charged ions along the composite membrane is facilitated. Moreover, the highly conjugated H_6hhtph linker, shown in Figure 19, enhances the conductivity among various molecules within the composite membrane. In addition, the Cu-MOF, used in the current study, is a highly porous graphene-like structure, with an average porosity of 1.55 (Hoppe et al., 2018). Compared with an average size of a typical H_2S molecule of 0.36 nm, the diffusion, and transportation of the H_2S molecules within the MOF molecules are, therefore, highly enhanced. It is, therefore, the synergistic effect of the highly connected molecules of the proposed nanocomposite membrane that explains its high efficiency and sensitivity toward H_2S gas. The high porosity of the MOF component of the composite membrane was previously proven to contribute to the passage of H_2S molecules within the composite membrane (Ali et al., 2021). The current findings support the contribution of the highly porous MOF structures in the construction of a gas sensor assembly. Moreover, it is believed that the homogeneous distribution of the graphene-like 2D Cu-MOF crystallites within the composite membrane explains the enhanced sensitivity towards H_2S molecules, as compared with PVA/IL membranes.
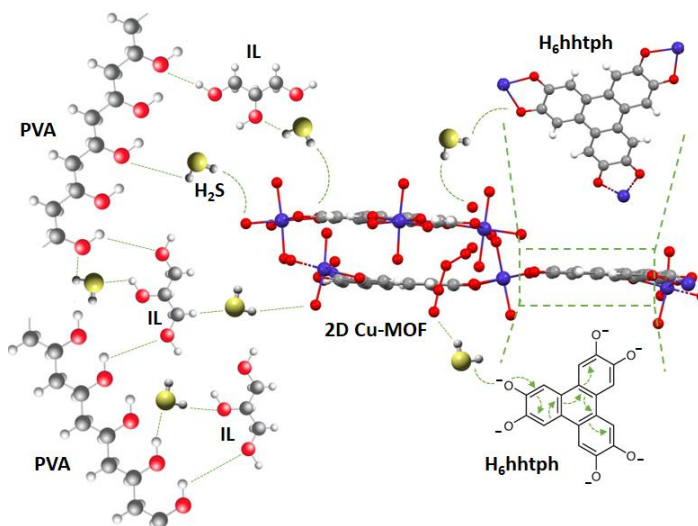
Figure 19: Illustration of the suggested H$_2$S gas sensing mechanism. All atoms are color-coded; Cu: purple, O: red, C: grey, H: white, S: yellow.

3.2.4 A Comparison of the Proposed Sensor Performance with the Reported Literature.

Table 2 demonstrates a comparison between the sensing performance of the Cu-MOF/PVA/IL sensor and previously reported sensors based on Cu and Cu-MOF materials for different target gases. The sensors' performance was evaluated by comparing different parameters, such as the operating temperature and the detection limit. It can be noticed that our proposed sensor combines having a low detection limit and low operating temperature, in addition to its high flexibility and easy fabrication technique, which nominate it as an excellent candidate to be deployed in practical industrial applications to detect H$_2$S gas.

Table 2 : A comparison of the Cu-MOF/PVA/IL sensor performance with the reported literature.

Sensor/Material	Operating Temp (°C)	Gas	Detection Limit	Refs.
Cu-MOF/PVA/IL	23°C	H_2S	1 ppm	This Work
Cu/Ni (HHTP)	RT	H_2S/NO	40–80 ppm	(Smith et al., 2016)
Cu-MOF	250°C	Acetone	50 ppm	(Arul et al., 2021)
		H_2/CO	20 ppm	
		CO_2/NH_3	200 ppm	
		CH_4	500 ppm	
		NO_2	1 ppm	
PVA-Semiconducting nanoparticles (CuO, $ZnFe_2O_4$, $CuFe_2O_4$, and WO_3) based sensors	80°C	H_2S	10 ppm	(Abu-Hani et al., 2017; Ayesh et al., 2016)
Pd and Pt NPs doped Cu-MOF	RT	NO_2	1 ppm	(Koo et al., 2019)

Chapter 4

Chapter 4: Conclusion and Future Work

4.1 Conclusion

This investigation demonstrates the potential of fabricating high-performance H_2S gas sensors. The flexible mixed matrix composite membranes were successfully prepared by doping ZnO Nps or Cu-MOF into an organic PVA polymer blended with IL. The fabricated membranes were investigated for their gas-sensing performance. The undoped PVA/IL membrane did not record any sensing towards H_2S gas, whereas the ZnO Nps and Cu-MOF doped membranes showed high sensitivity towards H_2S gas with a detection limit of 15 ppm and 1 ppm respectively, and a fast time response of 24 s and 12 s respectively at RT.

Considering this low operating temperature, the requirement of external heating elements was not required, hence the fabrication and operational costs are reduced. Along with the affinity towards H_2S, the membranes exhibit high selectivity, reproducibility, and long-term stability. Moreover, the composites of the proposed membranes are known to have no harm to the environment which makes them eco-friendly. Therefore, the proposed sensors have the potential to be implanted into electronic devices for potentially monitoring H_2S gas in real-time with high efficiency.

4.2 Future Work

This work has successfully achieved low power consumption, by working at room temperature. However, despite that the proposed sensors have excellent sensitivity and relatively fast response time, further enhancement is still possible to reduce the detection limit to the sub-ppm level, in addition to reducing the response time further.

That's why, our future work will focus on investigating different materials and morphologies that may help improve the sensing performance.

References

Abdullah, A. M., Aziz, S. B., & Saeed, S. R. (2021). Structural and electrical properties of polyvinyl alcohol (PVA): Methyl cellulose (MC) based solid polymer blend electrolytes inserted with sodium iodide (NaI) salt. *Arabian Journal of Chemistry*, *14*(11), 103388.

Abu-Hani, A. F., Awwad, F., Greish, Y. E., Ayesh, A. I., & Mahmoud, S. T. (2017). Design, fabrication, and characterization of low-power gas sensors based on organic-inorganic nano-composite. *Organic Electronics*, *42*, 284-292.

Alba-Martin, M., Firmager, T., Atherton, J., Rosamond, M. C., Ashall, D., Al Ghaferi, A., Ayesh, A., Gallant, A. J., Mabrook, M. F., & Petty, M. C. (2012). Improved memory behaviour of single-walled carbon nanotubes charge storage nodes. *Journal of Physics D: Applied Physics*, *45*(29), 295401.

Ali, A., Alzamly, A., Greish, Y. E., Bakiro, M., Nguyen, H. L., & Mahmoud, S. T. (2021). A Highly Sensitive and Flexible Metal–Organic Framework Polymer-Based H_2S Gas Sensor. *ACS Omega*.

Ali, F. I., Awwad, F., Greish, Y. E., Abu-Hani, A. F., & Mahmoud, S. T. (2020). Fabrication of low temperature and fast response H2S gas sensor based on organic-metal oxide hybrid nanocomposite membrane. *Organic Electronics*, *76*, 105486.

Ali, F. I., Awwad, F., Greish, Y. E., & Mahmoud, S. T. (2018). Hydrogen sulfide (H 2 S) gas sensor: A review. *IEEE Sensors Journal*, *19*(7), 2394-2407.

Ali, M., Wang, X., Haroon, U., Chaudhary, H. J., Kamal, A., Ali, Q., Saleem, M. H., Usman, K., Alatawi, A., & Ali, S. (2022). Antifungal activity of Zinc nitrate derived nano Zno fungicide synthesized from Trachyspermum ammi to control fruit rot disease of grapefruit. *Ecotoxicology and Environmental Safety*, *233*, 113311.

Allam, M., Ayesh, A. I., Mohsin, M. A., & Haik, Y. (2013). Physical properties of PVA doped with algal glycerol. *Journal of Applied Polymer Science*, *130*(6), 4482-4489.

Arul, C., Moulaee, K., Donato, N., Iannazzo, D., Lavanya, N., Neri, G., & Sekar, C. (2021). Temperature modulated Cu-MOF based gas sensor with dual selectivity to acetone and NO_2 at low operating temperatures. *Sensors and Actuators B: Chemical*, *329*, 129053.

Ayesh, A. I., Abu-Hani, A. F., Mahmoud, S. T., & Haik, Y. (2016). Selective H_2S sensor based on CuO nanoparticles embedded in organic membranes. *Sensors and Actuators B: Chemical*, *231*, 593-600.

Ayesh, A. I., Mohsin, M. A., Haik, M. Y., & Haik, Y. (2012). Investigations on electrical properties of poly (vinyl alcohol) doped with 1-methyl-3-n-decyl-imidazolium bromide ionic liquid. *Current Applied Physics*, *12*(4), 1223-1228.

Banica, F.-G. (2012). *Chemical sensors and biosensors: fundamentals and applications*. John Wiley & Sons.

Campbell, M. G., Liu, S. F., Swager, T. M., & Dincă, M. (2015). Chemiresistive sensor arrays from conductive 2D metal–organic frameworks. *Journal of the American Chemical Society*, *137*(43), 13780-13783.

Campbell, M. G., Sheberla, D., Liu, S. F., Swager, T. M., & Dincă, M. (2015). Cu_3(hexaiminotriphenylene)$_2$: An electrically conductive 2D metal–organic framework for chemiresistive sensing. *Angewandte Chemie International Edition*, *54*(14), 4349-4352.

Chen, E.-X., Yang, H., & Zhang, J. (2014). Zeolitic imidazolate framework as formaldehyde gas sensor. *Inorganic Chemistry*, *53*(11), 5411-5413.

Chen, X., Behboodian, R., Bagnall, D., Taheri, M., & Nasiri, N. (2021). Metal-Organic-Frameworks: Low Temperature Gas Sensing and Air Quality Monitoring. *Chemosensors*, *9*(11), 316.

COBIANU, C., STRATULAT, A., SERBAN, B., BREZEANU, M., & BUIU, O. (2016). Sonochemical syntheses of metal oxide nanocomposites for gas sensing. *Annals of the Academy of Romanian Scientists, Series on Science and Technology of Information*, *9*(1), 5-12.

Çolak, H., & Karaköse, E. (2019). Synthesis and characterization of different dopant (Ge, Nd, W)-doped ZnO nanorods and their CO_2 gas sensing applications. *Sensors and Actuators B: Chemical*, *296*, 126629.

Culshaw, B. (1983). Optical systems and sensors for measurement and control. *Journal of Physics E: Scientific Instruments*, *16*(10), 978.

Diep, V. M., & Armani, A. M. (2016). Flexible light-emitting nanocomposite based on ZnO nanotetrapods. *Nano Letters*, *16*(12), 7389-7393.

Ding, P., Xu, D., Dong, N., Chen, Y., Xu, P., Zheng, D., & Li, X. (2020). A high-sensitivity H_2S gas sensor based on optimized ZnO-ZnS nano-heterojunction sensing material. *Chinese Chemical Letters*, *31*(8), 2050-2054.

Geng, X., Zhang, C., & Debliquy, M. (2016). Cadmium sulfide activated zinc oxide coatings deposited by liquid plasma spray for room temperature nitrogen dioxide detection under visible light illumination. *Ceramics International*, *42*(4), 4845-4852.

Ghosh, A., Zhang, C., Shi, S., & Zhang, H. (2019). High temperature CO_2 sensing and its cross-sensitivity towards H_2 and CO gas using calcium doped ZnO thin film coated langasite SAW sensor. *Sensors and Actuators B: Chemical*, *301*, 126958.

Ghosh, S., Adak, D., Bhattacharyya, R., & Mukherjee, N. (2017). ZnO/γ-Fe_2O_3 charge transfer interface toward highly selective H_2S sensing at a low operating temperature of 30°C. *ACS Sensors*, *2*(12), 1831-1838.

Gupta, S. P., Pawbake, A. S., Sathe, B. R., Late, D. J., & Walke, P. S. (2019). Superior humidity sensor and photodetector of mesoporous ZnO nanosheets at room temperature. *Sensors and Actuators B: Chemical*, *293*, 83-92.

Haik, Y., Ayesh, A. I., & Mohsin, M. A. (2014). Semiconducting polymer. In: Google Patents.

Hittini, W., Greish, Y. E., Qamhieh, N. N., Alnaqbi, M. A., Zeze, D., & Mahmoud, S. T. (2020). Ultrasensitive and low temperature gas sensor based on electrospun organic-inorganic nanofibers. *Organic Electronics*, *81*, 105659.

Hodgkinson, J., & Tatam, R. P. (2012). Optical gas sensing: a review. *Measurement science and technology*, *24*(1), 012004.

Hoppe, B., Hindricks, K. D., Warwas, D. P., Schulze, H. A., Mohmeyer, A., Pinkvos, T. J., Zailskas, S., Krey, M. R., Belke, C., & König, S. (2018). Graphene-like metal–organic frameworks: morphology control, optimization of thin film electrical conductivity and fast sensing applications. *CrystEngComm*, *20*(41), 6458-6471.

Hsu, C.-L., Chang, L.-F., & Hsueh, T.-J. (2017). Light-activated humidity and gas sensing by ZnO nanowires grown on LED at room temperature. *Sensors and Actuators B: Chemical*, *249*, 265-277.

Jayarambabu, N., Kumari, B. S., Rao, K. V., & Prabhu, Y. (2014). Germination and growth characteristics of mungbean seeds (Vigna radiata L.) affected by synthesized zinc oxide nanoparticles. *International Journal of Current Engineering and Technology*, *4*(5), 2347-5161.

Jiang, X., Kim, K., Zhang, S., Johnson, J., & Salazar, G. (2013). High-temperature piezoelectric sensing. *Sensors*, *14*(1), 144-169.

Jiang, Y., Decker, S., Mohs, C., & Klabunde, K. J. (1998). Catalytic solid state reactions on the surface of nanoscale metal oxide particles. *Journal of Catalysis*, *180*(1), 24-35.

Josh, V., Haik, M. Y., Ayesh, A. I., Mohsin, M. A., & Haik, Y. (2013). Electrical properties of sorbitol-doped poly (vinyl alcohol)–poly (acrylamide-co-acrylic acid) polymer membranes. *Journal of Applied Polymer Science*, *128*(6), 3861-3869.

Joshi, N., Hayasaka, T., Liu, Y., Liu, H., Oliveira, O. N., & Lin, L. (2018). A review on chemiresistive room temperature gas sensors based on metal oxide nanostructures, graphene and 2D transition metal dichalcogenides. *Microchimica Acta*, *185*(4), 1-16.

Kang, Y., Yu, F., Zhang, L., Wang, W., Chen, L., & Li, Y. (2021). Review of ZnO-based nanomaterials in gas sensors. *Solid State Ionics*, *360*, 115544.

Kohl, D. (2001). Function and applications of gas sensors. *Journal of Physics D: Applied Physics*, *34*(19), R125.

Kolhe, P. S., Shinde, A. B., Kulkarni, S., Maiti, N., Koinkar, P. M., & Sonawane, K. M. (2018). Gas sensing performance of Al doped ZnO thin film for H_2S detection. *Journal of Alloys and Compounds*, *748*, 6-11.

Koo, W. T., Kim, S. J., Jang, J. S., Kim, D. H., & Kim, I. D. (2019). Catalytic metal nanoparticles embedded in conductive metal–organic frameworks for chemiresistors: highly active and conductive porous materials. *Advanced Science*, *6*(21), 1900250.

Korotcenkov, G., & Cho, B. (2012). The role of grain size on the thermal instability of nanostructured metal oxides used in gas sensor applications and approaches for grain-size stabilization. *Progress in Crystal Growth and Characterization of Materials*, *58*(4), 167-208.

Kramer, K. E., Rose-Pehrsson, S. L., Hammond, M. H., Tillett, D., & Streckert, H. H. (2007). Detection and classification of gaseous sulfur compounds by solid electrolyte cyclic voltammetry of cermet sensor array. *Analytica chimica acta*, *584*(1), 78-88.

Kumar, M., Bhatt, V., Abhyankar, A. C., Yun, J.-H., & Jeong, H.-J. (2020). Multifunctional dumbbell-shaped ZnO based temperature-dependent UV photodetection and selective H_2 gas detection. *International Journal of Hydrogen Energy*, *45*(29), 15011-15025.

Kumar, R. S., Kumar, S. S., & Kulandainathan, M. A. (2013). Efficient electrosynthesis of highly active $Cu_3(BTC)_2$-MOF and its catalytic application to chemical reduction. *Microporous and Mesoporous Materials*, *168*, 57-64.

Lei, N., Li, P., Xue, W., & Xu, J. (2011). Simple graphene chemiresistors as pH sensors: fabrication and characterization. *Measurement science and technology*, *22*(10), 107002.

Liang, X., He, Y., Liu, F., Wang, B., Zhong, T., Quan, B., & Lu, G. (2007). Solid-state potentiometric H2S sensor combining NASICON with Pr6O11-doped SnO2 electrode. *Sensors and Actuators B: Chemical*, *125*(2), 544-549.

Liu, G., Wang, Y., Xue, Q., Wen, Y., Hong, X., & Ullah, K. (2021). TiO₂/Cu-MOF/PPy composite as a novel photocatalyst for decomposition of organic dyes. *Journal of Materials Science: Materials in Electronics*, *32*(4), 4097-4109.

Liu, X., Cheng, S., Liu, H., Hu, S., Zhang, D., & Ning, H. (2012). A survey on gas sensing technology. *Sensors*, *12*(7), 9635-9665.

Lupan, O., Postica, V., Gröttrup, J., Mishra, A. K., De Leeuw, N. H., Carreira, J. F., Rodrigues, J., Ben Sedrine, N., Correia, M. R., & Monteiro, T. (2017). Hybridization of zinc oxide tetrapods for selective gas sensing applications. *ACS Applied Materials & Interfaces*, *9*(4), 4084-4099.

Majhi, S. M., Mirzaei, A., Kim, H. W., Kim, S. S., & Kim, T. W. (2021). Recent advances in energy-saving chemiresistive gas sensors: A review. *Nano Energy*, *79*, 105369.

Mashrai, A., Khanam, H., & Aljawfi, R. N. (2017). Biological synthesis of ZnO nanoparticles using C. albicans and studying their catalytic performance in the synthesis of steroidal pyrazolines. *Arabian Journal of Chemistry*, *10*, S1530-S1536.

McDonagh, C., Burke, C. S., & MacCraith, B. D. (2008). Optical chemical sensors. *Chemical reviews*, *108*(2), 400-422.

Nam, K. W., Park, S. S., Dos Reis, R., Dravid, V. P., Kim, H., Mirkin, C. A., & Stoddart, J. F. (2019). Conductive 2D metal-organic framework for high-performance cathodes in aqueous rechargeable zinc batteries. *Nature Communications*, *10*(1), 1-10.

Nanto, H., Dougami, N., Mukai, T., Habara, M., Kusano, E., Kinbara, A., Ogawa, T., & Oyabu, T. (2000). A smart gas sensor using polymer-film-coated quartz resonator microbalance. *Sensors and Actuators B: Chemical*, *66*(1-3), 16-18.

Narayana, A., Bhat, S. A., Fathima, A., Lokesh, S., Surya, S. G., & Yelamaggad, C. (2020). Green and low-cost synthesis of zinc oxide nanoparticles and their application in transistor-based carbon monoxide sensing. *RSC Advances*, *10*(23), 13532-13542.

Navaneethan, M., Patil, V., Ponnusamy, S., Muthamizhchelvan, C., Kawasaki, S., Patil, P., & Hayakawa, Y. (2018). Sensitivity enhancement of ammonia gas sensor based on Ag/ZnO flower and nanoellipsoids at low temperature. *Sensors and Actuators B: Chemical*, *255*, 672-683.

Niranjan, R., Chaudhary, V., Mulla, I., & Vijayamohanan, K. (2002). A novel hydrogen sulfide room temperature sensor based on copper nanocluster functionalized tin oxide thin films. *Sensors and Actuators B: Chemical*, *85*(1-2), 26-32.

Occupational Safety and Health Administration. *Hydrogen sulfide*. retrieved from https://www.osha.gov/hydrogen-sulfide/hazards accessed on 10/04/2022

Örnek, Ö., & Karlık, B. (2012). An overview of metal oxide semiconducting sensors in electronic nose applications. Proc. of the 3rd International Symposium on Sustainable Development,

Pandey, S. K., Kim, K.-H., & Tang, K.-T. (2012). A review of sensor-based methods for monitoring hydrogen sulfide. *TrAC Trends in Analytical Chemistry*, *32*, 87-99.

Park, C., & Kim, I.-D. (2020). Bimetallic Nanoparticles-Stabilized Conductive Metal-Organic Frameworks for Superior Chemiresistors. ECS Meeting Abstracts,

Park, S., An, S., Mun, Y., & Lee, C. (2013). UV-enhanced NO_2 gas sensing properties of SnO_2-core/ZnO-shell nanowires at room temperature. *ACS Applied Materials & Interfaces*, *5*(10), 4285-4292.

Patil, P., Gaikwad, G., Patil, D., & Naik, J. (2016). Synthesis of 1-D ZnO nanorods and polypyrrole/1-D ZnO nanocomposites for photocatalysis and gas sensor applications. *Bulletin of Materials Science*, *39*(3), 655-665.

Pohle, R., Tawil, A., Davydovskaya, P., & Fleischer, M. (2011). Metal organic frameworks as promising high surface area material for work function gas sensors. *Procedia Engineering*, *25*, 108-111.

Rawool, C. R., & Srivastava, A. K. (2019). A dual template imprinted polymer modified electrochemical sensor based on Cu metal organic framework/mesoporous carbon for highly sensitive and selective recognition of rifampicin and isoniazid. *Sensors and Actuators B: Chemical*, *288*, 493-506.

Ristić, M., Musić, S., Ivanda, M., & Popović, S. (2005). Sol–gel synthesis and characterization of nanocrystalline ZnO powders. *Journal of Alloys and Compounds*, *397*(1-2), L1-L4.

Roy, A. S., Gupta, S., Sindhu, S., Parveen, A., & Ramamurthy, P. C. (2013). Dielectric properties of novel PVA/ZnO hybrid nanocomposite films. *Composites Part B: Engineering*, *47*, 314-319.

Sciau, P. (2012). Nanoparticles in ancient materials: the metallic lustre decorations of medieval ceramics.

Scozzari, A. (2008). Electrochemical sensing methods: a brief review. *Algal Toxins: Nature, Occurrence, Effect and Detection*, 335-351.

Shewale, P. S., & Yun, K.-S. (2020). Synthesis and characterization of Cu-doped ZnO/RGO nanocomposites for room-temperature H_2S gas sensor. *Journal of Alloys and Compounds*, *837*, 155527.

Singh, P., Kumar, A., Kaushal, A., Kaur, D., Pandey, A., & Goyal, R. (2008). In situ high temperature XRD studies of ZnO nanopowder prepared via cost effective ultrasonic mist chemical vapour deposition. *Bulletin of Materials Science*, *31*(3), 573-577.

Smith, M. K., Jensen, K. E., Pivak, P. A., & Mirica, K. A. (2016). Direct self-assembly of conductive nanorods of metal–organic frameworks into chemiresistive devices on shrinkable polymer films. *Chemistry of Materials*, *28*(15), 5264-5268.

Toda, K., Ohira, S.-I., Tanaka, T., Nishimura, T., & Dasgupta, P. K. (2004). Field instrument for simultaneous large dynamic range measurement of atmospheric hydrogen sulfide, methanethiol, and sulfur dioxide. *Environmental science & technology*, *38*(5), 1529-1536.

Varga, A., Bozóki, Z., Szakáll, M., & Szabó, G. (2006). Photoacoustic system for on-line process monitoring of hydrogen sulfide (H2S) concentration in natural gas streams. *Applied Physics B*, *85*(2), 315-321.

Varghese, S. S., Lonkar, S., Singh, K., Swaminathan, S., & Abdala, A. (2015). Recent advances in graphene based gas sensors. *Sensors and Actuators B: Chemical*, *218*, 160-183.

Wang, J., Xia, Y., Zhao, H., Wang, G., Xiang, L., Xu, J., & Komarneni, S. (2017). Oxygen defects-mediated Z-scheme charge separation in g-C_3N_4/ZnO photocatalysts for enhanced visible-light degradation of 4-chlorophenol and hydrogen evolution. *Applied Catalysis B: Environmental*, *206*, 406-416.

Wang, P., Dong, T., Jia, C., & Yang, P. (2019). Ultraselective acetone-gas sensor based ZnO flowers functionalized by Au nanoparticle loading on certain facet. *Sensors and Actuators B: Chemical*, *288*, 1-11.

Wang, X., Ding, B., Yu, J., Wang, M., & Pan, F. (2009). A highly sensitive humidity sensor based on a nanofibrous membrane coated quartz crystal microbalance. *Nanotechnology*, *21*(5), 055502.

Wang, X., Li, S., Xie, L., Li, X., Lin, D., & Zhu, Z. (2020). Low-temperature and highly sensitivity H_2S gas sensor based on ZnO/CuO composite derived from bimetal metal-organic frameworks. *Ceramics International*, *46*(10), 15858-15866.

Wang, X., Wang, Y., Tian, F., Liang, H., Wang, K., Zhao, X., Lu, Z., Jiang, K., Yang, L., & Lou, X. (2015). From the surface reaction control to gas-diffusion control: the synthesis of hierarchical porous SnO_2 microspheres and their gas-sensing mechanism. *The Journal of Physical Chemistry C*, *119*(28), 15963-15976.

Wang, Y., & Yan, H. (2002). Solid polymer electrolyte-based hydrogen sulfide sensor. *Sensors and Actuators B: Chemical*, *87*(1), 115-121.

Wei, W., Zhao, J., Shi, S., Lin, H., Mao, Z., Zhang, F., & Qu, F. (2020). Boosting ppb-level triethylamine sensing of ZnO: adjusting proportions of electron donor defects. *Journal of Materials Chemistry C*, *8*(20), 6734-6742.

Xu, J., Pan, Q., & Qin, J. (2000). Sensing characteristics of double layer film of ZnO. *Sensors and Actuators B: Chemical*, *66*(1-3), 161-163.

Yao, M. S., Lv, X. J., Fu, Z. H., Li, W. H., Deng, W. H., Wu, G. D., & Xu, G. (2017). Layer-by-layer assembled conductive metal–organic framework nanofilms for room-temperature chemiresistive sensing. *Angewandte Chemie*, *129*(52), 16737-16741.

Yao, M. S., Zheng, J. J., Wu, A. Q., Xu, G., Nagarkar, S. S., Zhang, G., Tsujimoto, M., Sakaki, S., Horike, S., & Otake, K. (2020). A Dual-Ligand Porous Coordination Polymer Chemiresistor with Modulated Conductivity and Porosity. *Angewandte Chemie International Edition*, *59*(1), 172-176.

Yogeswaran, U., & Chen, S.-M. (2008). A review on the electrochemical sensors and biosensors composed of nanowires as sensing material. *Sensors*, *8*(1), 290-313.

Yourong, W., Heqing, Y., & E'feng, W. (2001). The electrochemical oxidation and the quantitative determination of hydrogen sulfide on a solid polymer electrolyte-based system. *Journal of Electroanalytical Chemistry*, *497*(1-2), 163-167.

Yu, C., Wang, Y., Hua, K., Xing, W., & Lu, T. (2002). Electrochemical H2S sensor with H2SO4 pre-treated Nafion membrane as solid polymer electrolyte. *Sensors and Actuators B: Chemical*, *86*(2-3), 259-265.

Yu, Z., Gao, J., Xu, L., Liu, T., Liu, Y., Wang, X., Suo, H., & Zhao, C. (2020). Fabrication of Lettuce-Like ZnO Gas Sensor with Enhanced H_2S Gas Sensitivity. *Crystals*, *10*(3), 145.

Yuan, H., Aljneibi, S. A. A. A., Yuan, J., Wang, Y., Liu, H., Fang, J., Tang, C., Yan, X., Cai, H., & Gu, Y. (2019). ZnO nanosheets abundant in oxygen vacancies derived from metal-organic frameworks for ppb-level gas sensing. *Advanced Materials*, *31*(11), 1807161.

Zhang, B., Li, M., Song, Z., Kan, H., Yu, H., Liu, Q., Zhang, G., & Liu, H. (2017). Sensitive H_2S gas sensors employing colloidal zinc oxide quantum dots. *Sensors and Actuators B: Chemical*, *249*, 558-563.

Zhang, D., Fan, X., Hao, X., & Dong, G. (2019). Facile fabrication of polyaniline nanocapsule modified zinc oxide hexagonal microdiscs for H_2S gas sensing applications. *Industrial & Engineering Chemistry Research*, *58*(5), 1906-1913.

Zhang, J., Qin, Z., Zeng, D., & Xie, C. (2017). Metal-oxide-semiconductor based gas sensors: screening, preparation, and integration. *Physical Chemistry Chemical Physics*, *19*(9), 6313-6329.

Zhang, J., Zhao, B., Pan, Z., Gu, M., & Punnoose, A. (2015). Synthesis of ZnO nanoparticles with controlled shapes, sizes, aggregations, and surface complex compounds for tuning or switching the photoluminescence. *Crystal Growth & Design*, *15*(7), 3144-3149.

Zhang, S., & Yu, F. (2011). Piezoelectric materials for high temperature sensors. *Journal of the American Ceramic Society*, *94*(10), 3153-3170.

Zhao, S., Shen, Y., Yan, X., Zhou, P., Yin, Y., Lu, R., Han, C., Cui, B., & Wei, D. (2019). Complex-surfactant-assisted hydrothermal synthesis of one-dimensional ZnO nanorods for high-performance ethanol gas sensor. *Sensors and Actuators B: Chemical*, *286*, 501-511.

Zhu, L., Li, Y., & Zeng, W. (2018). Hydrothermal synthesis of hierarchical flower-like ZnO nanostructure and its enhanced ethanol gas-sensing properties. *Applied Surface Science*, *427*, 281-287.

Zhu, L., & Zeng, W. (2017). A novel coral rock-like ZnO and its gas sensing. *Materials Letters*, *209*, 244-246.

List of Publications

Ali, A., AlTakroori, H. H.D , Greish, Y. E., Alzamly, A., Siddig, L. A., Qamhieh, N., & Mahmoud, S. T. (2022). Flexible Cu_3 (HHTP) $_2$ MOF Membranes for Gas Sensing Application at Room Temperature. Nanomaterials, 12(6), 913. https://doi.org/10.3390/nano12060913 (IF=5.076)

AlTakroori, H. H. D., Ali, A., Greish, Y. E., Qamhieh, N., & Mahmoud, S. T. (2022). Organic/Inorganic-Based Flexible Membrane for a Room-Temperature Electronic Gas Sensor. Nanomaterials, 12(12), 2037. http://doi.org/10.3390/nano12122037 (IF=5.076)

UAE UNIVERSITY MASTER THESIS NO. 2022:24

This work aims at developing high-performance gas sensors with enhanced sensitivity, fast response time, and low operating temperature. The fabricated sensors showed high sensitivity toward hydrogen sulfide (H_2S) gas, and fast response time at room temperature. Considering this low operating temperature, external heating elements are not required hence the fabrication and operational costs are reduced. The sensors also showed excellent repeatability, long-term stability, and selectivity toward H_2S gas among other gases. Therefore, this study demonstrates the potential of fabricating high-performance gas sensors for monitoring H_2S gas in real-time with high efficiency.

Husam H.D. AlTakroori received his Master of Science in Physics from the Department of Physics, College of Science and his Bachelor of Science in Applied Physics from the College of Science, Palestine Polytechnic University, Palestine.

www.uaeu.ac.ae